Amplitude and Phase Control in Active Suppression of Combustion Instability

Dimitry Gorinevsky*, Nick Overman†, and Jerry Goeke†

***Abstract*— This paper provides stability analysis for phase shifting active combustion control system where modulation of the fuel flow is used to suppress thermo-acoustic instability. The analysis is based on Krylov-Bogolubov averaged model for the oscillations with the external periodic forcing. The amplitude dynamics and phase dynamics are described by nonlinear first order models. The control inputs are the amplitude and phase of forcing (fuel modulation). The analysis demonstrates that phase dynamics and amplitude dynamics are each unstable in the desired target regime. Practical stabilizing control approaches and their limitations in the presence of feedback delays are discussed and analyzed. The analysis in this paper is verified in detailed simulations and validated in experiments with a jet engine scale combustor rig.**

I. INTRODUCTION

Operating gas turbines in fuel-lean regime could reduce NOX emissions and thermal load on the system. Unfortunately, lean combustion creates conditions for thermo-acoustic instability, causing undesirable pressure and thermal oscillations in the combustion chamber. These oscillations can be reduced by modulating fuel flow at their frequency. The approach is known as phase shifting control since the modulation phase must be shifted compared to the observed oscillation phase to ensure the suppression. This paper analyzes stability issues caused by the delays in the phase shifting control loop.

The phase shifting control system considered in this work is illustrated in Figure 1. Earlier work included similar design and analysis elements. On the far right, the spring and mass depicts an oscillator driven by thermo-acoustic self-excitation mechanism. The oscillator state is measured by a sensor (optical or acoustic pressure). The actuator, such as a fuel flow modulation valve, applies control effort influencing the oscillator. The sensors and the actuator are connected to a digital control system shown on the left in Figure 1. The sensor data is sampled and digitized, then used to estimate the phase and amplitude of the oscillations. The phase and amplitude control logic uses the estimated phase and amplitude to compute the actuation parameters (the frequency, phase and amplitude of the valve modulation).

Active combustion control systems (ACCS) using phase shifting approach is a well developed research area. This paper does not have space to survey it in sufficient detail. The surveys can be found in [1], [9]. Phase shifting control is dominant in practical ACCS, see [1], [6], [9]. Among all published ACCS work there are very few realistic scale tirbine combustor demonstrations such as [2], [10], [12], [13], [18]. This is likely because of the cost and comprehensiveness of the real turbomachine scale experimental work.

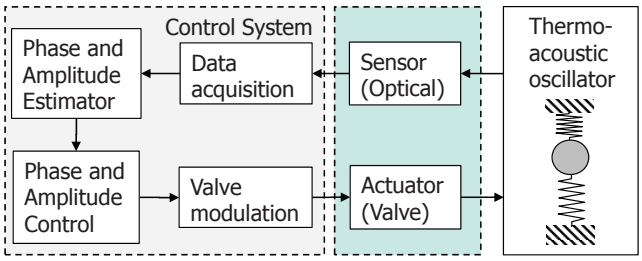

Fig. 1. Overview of active combustion control system

Another reason why full-scale combustors with active control have not been implemented in jet engines is the lack of reliable liquid-fuel actuators that can continuously pulse at a very high acoustic frequencies with high authority, see [6]. The earlier practical demonstrations of ACCS [15], [10], [17], [18] were in rocket engines and ground turbines using gas fuel. This work was initially motivated by our project in a practical scale demonstration of ACCS for a jet engine combustor using a new valve actuator with high bandwidth and high authority, see [14].

In the experiments, it became apparent that achievable acoustic oscillation suppression is limited by control issues related to the delay in the phase and amplitude feedback. These issues are fundamental, can be explained using a simple model, and, to the best of our knowledge, were not adequately described in the published ACCS literature.

One issue is with the phase shift error. The oscillation frequency is influenced by the modulation and otherwise changes with time. The transport delay in fuel lines can be many periods of oscillation and the frequency change can significantly modify the effective phase shift. Thus, a feedback correction of the phase shift is necessary; this feedback is susceptible to the loop delay.

Another issue is with the modulation amplitude control. The experiments and simulations show that fixed amplitude modulation with large enough control authority could reduce the oscillations till the phase tracking is impossible. To avoid cyclic loss of control and increase of the oscillations the modulation amplitude must be controlled; however, the amplitude feedback is susceptible to the feedback loop delay.

Depending on the intensity of the instability and the feed-

This work was supported by Air Force Research Laboratory Contract "Active Combustion Control Systems for Military Aircraft"

*Mitek Analytics LLC, Palo Alto, CA 94306, dimitry@mitekan.com and Dept. of Electical Engineering, Stanford University, gorin@stanford.edu

†Turbine Fuel Technologies, Goodrich Corp., West Des Moines, Iowa 50265

back delay, it might be impossible to reduce the oscillation amplitude substantially (by more than half). This appears to be a fundamental issue with ACCS.

Understanding these issues requires analysis of controlled dynamics of the amplitude and phase. The phase shifting approach recognizes that control authority and bandwidth are limited and attempts to drive down the oscillation amplitude over many cycles. The cycle-to-cycle evolution of the oscillations can be analyzed using averaging. The averaging approach is applicable no matter what the sensors sampling and actuator control scheme is (our experimental work uses sophisticated multirate sampling of measurements and actuator commands). For many of the alternative published ACCS algorithms, the averaged effect on the oscillations is not that much different from the phase shifting control.

The fundamental limitations of the ACCS, including the feedback delay issue were noted in [3] using frequency domain reasoning that was focused on a specific example and characterized the nonlinearities through a describing function. This paper shows that the limitations exist in a simple averaged dynamics model with just two states. Related work in [2], [4] used averaging methods for analysis of closed loop amplitude dynamics for ACCS. This paper adopts a simple Van der Pol model for themoacoustic oscillations discussed in [4]. In [2], [4] the relative phase is assumed fixed and amplitude dynamics does not include the feedback loop delay.

The main novelty of this paper is in analysing averaged dynamics and control of phase and amplitude of the thermo-acoustic oscillations taking into account feedback delay. The analysis is based on a slow time scale model for coupled phase and amplitude dynamics of the oscillation obtained using Krylov-Bogolyubov (K-B) averaging method. The model incorporates the self-excitation and harmonic forcing. The detailed contributions are as follows

1) We present theoretical analysis of the phase shifting control limitations caused by the delay in the feedback loop. These limitations are fundamental enough to exist even for a very simple model of the problem.
2) The paper demonstrates that the open-loop relative phase dynamics in phase shifting control are unstable.
3) The paper shows that the open-loop amplitude dynamics are unstable as well in the most desirable oscillation suppression regime.
4) The theoretical analysis is verified in comprehensive simulations and validated in experiments.

The paper outline is as follows. Section II derives the averaged model for amplitude and phase control using the K-B averaging. Section III provides the key control analysis contributions of this paper for stability of the phase and amplitude control with feedback delay. In Section IV we introduce a multirate phase lock loop filter estimating the amplitude, frequency, and phase from the acquired process data. Section IV described the comprehensive simulation model. The theoretical analysis is verified in closed loop simulation. Finally, Section VI reports the experimental results.

II. Idealized Model for Amplitude and Phase Dynamics

As a starting point, we consider an idealized model for the amplitude and phase dynamics in phase shift control. The published ACCS work for realistic scale liquid-fuel combustors is in control of one (main) oscillation mode using fixed amplitude of the fuel flow modulation. A single mode was controlled in our experiments and a single-mode model is considered below. This is, perhaps, the simplest possible model of ACCS retaining the salient features of the problem. We believe that the issues identified for this simple model are fundamental to the problem.

A. Oscillations model

A simple model for the thermo-acoustic instability is provided by Van der Pol equation. Several earlier papers used such a model for the combustion instability, for instance, see [4]. Consider the following model

$$\ddot{p}(t) + \Omega^2 p(t) = q_{int}(p(t), \dot{p}(t)) + q_{ext}(t) + e(t), \quad (1)$$

$$q_{int}(p, \dot{p}) = \mu\Omega(1 - p^2/p_c^2)\dot{p}, \quad (2)$$

where $p(t)$ is the variation of the combustion chamber pressure and $p_c(t)$ is a scaling constant (half of the limit cycle magnitude). The l.h.s. (left hand side) of (1) describes a harmonic oscillator with natural frequency Ω. Three forces act on the oscillator. The internal excitation q_{int} (2) describes the thermo-acoustic effects leading to instability. In accordance to a Galerkin model described in [8], the internal excitation corresponds to the time derivative of the heat release in the oscillation. The time derivatives of heat release rate and $\dot{p}$ are correlated in the same way as the heat release rate and pressure p in the Rayleigh's criterion. For small amplitude, $p^2/p_c^2 < 1$ and the energy is added at each oscillation cycle. For large amplitude, $p^2/p_c^2 > 1$ and the energy is removed. A more accurate model of thermo-acoustic effects might give a different curve for added energy vs amplitude; yet, the pattern of energy added at small amplitude and removed at large amplitude would be the same.

The analysis below assumes that the excitation intensity is small, $\mu \ll 1$. This means that the relative amount of energy added or subtracted at each oscillation cycle is small and it takes many cycles for the steady oscillations to develop.

The white noise $e(t)$ models random factors, such as the turbulence in combustor air flow. The noise was included in the simulations. The averaging and control analysis below do not take the noise $e(t)$ into account.

The external forcing function q_{ext} describes the effect of combustor fuel flow modulation on the pressure oscillations,

$$q_{ext}(t) = -ap_c \cos(wt + \psi), \quad (3)$$

where a is the normalized modulation amplitude, w is the modulation frequency, and ψ is the modulation phase at time.

It is assumed that the forced oscillations can be described as $p(t) = Ap_c \sin(wt+\phi)$, where A, w, and ϕ are amplitude, frequency, and phase of the oscillations. In what follows, A and ϕ can be (slowly) time varying, while w is constant.

B. Averaged equations

Applying the averaging method of Krylov-Bogolyubov (K-B) [5] allows to develop analytical expressions for dynamics of amplitude and phase of the oscillations.

The second order system (1) has two states p, and $\dot{p}$. To apply the K-B method consider the variable change $\{p(t), \dot{p}(t)\} \to \{A(t), \phi(t)\}$

$$p = Ap_c \sin(wt + \phi) \quad (4)$$
$$\dot{p} = Ap_c w \cos(wt + \phi) \quad (5)$$

Differentiating (5) yields

$$\ddot{p}/p_c = -Aw^2 \sin(wt+\phi) - Aw\dot{\phi} \sin(wt+\phi) + \dot{A}w \cos(wt+\phi)$$

By substituting this expression, (4), and (5) into (1), (2), (3) we get a single equation including the terms with $\dot{A}\cos(wt + \phi)$ and $\dot{\phi}\sin(wt + \phi)$. The first approximation of the K-B method is obtained by collecting the direct and the quadrature terms for the main harmonic. This can be done by multiplying the derived equation by $\sin(wt + \phi)$ and $\cos(wt + \phi)$ and computing the average (the integral) over the oscillation period $[t - 2\pi/w, t]$. The averaging approximation assumes that change of A and ϕ over a single oscillation period is small and because of that A and ϕ can be treated as constants when integrating. (For example, the average of $A\sin^2(wt + \psi)$ is computed as $\frac{1}{2}A$.). The averaging approximation implies the assumption that the forcing frequency w is close to the frequency of the oscillations in the system.

The averaged dynamics equations are

$$\dot{A}w = \mu\Omega A w(1 - \frac{1}{4}A^2) - a\cos(\psi - \phi), \quad (6)$$
$$\dot{\phi}w = \Omega^2 - w^2 - aA^{-1}\sin(\psi - \phi), \quad (7)$$

where A and ϕ are the states of the controlled system. The amplitude a, frequency w, and phase ψ of the harmonic forcing (3) are the control handles.

The averaged model (6), (7), allows quantifying the instability, the limit cycle of the oscillations, and closed-loop effects of phased control on the oscillation amplitude and phase.

Averaging methods were recently used for analysis of phase shifting control and sinusoidal disturbance rejection, though in different formulations, in [2], [4], [11]. The Rayleigh's criterion that is well known in analysis of thermo-acoustic combustion instabilities can be obtained as a special case of the K-B averaged equation for energy. The main novelty of this paper is in the analysis of averaged phase dynamics (7) and the analysis of the feedback control for the phase and amplitude including the influence of the delay.

C. Amplitude dynamics

Consider amplitude dynamics (6) for the forced oscillations and denote $U = 4a\cos(\psi - \phi)/(\mu\Omega)$. Then (6) yields

$$\dot{A} = \frac{1}{4}\mu\Omega(4A - A^3 - U), \quad (8)$$

where U is the new control variable. This subsection assumes that $U = \text{const}$. Assuming that $\cos(\psi - \phi) \approx 1$, this means that modulation amplitude $a \approx \text{const}$.

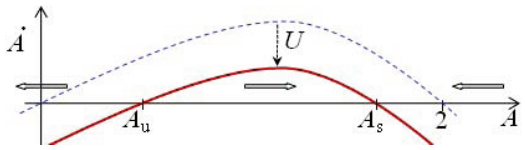

Fig. 2. Amplitude dynamics and its equilibria

The dashed line in Figure 2 illustrates amplitude dynamics in the absence of control, for $U = 0$. For $A < 2$ we have $\dot{A} > 0$ and the amplitude grows. For $A > 2$, the amplitude is diminishing, the rate $\dot{A} < 0$. Thus, $A = 2$ is a stable limit cycle.

Applying constant control U moves the entire $\dot{A}(A)$ curve down. If $U > U_{max} = 16/(3\sqrt{3}) \approx 3.0792$, then always $\dot{A} < 0$ and the amplitude A in (6) is driven to zero. This is unacceptable because if A is below the noise level, tracking of the oscillation phase becomes impossible. Section III-A below explains that small A also leads to instability of phase control. Thus, the goal of amplitude control is to maintain small fixed amplitude of the sustained oscillations.

For $U < U_{max}$, there are two limit cycles (equilibria) characterized by the positive roots of the cubic equation $4A - A^3 - U = 0$ (the solid line in Figure 2). As one can see from Figure 2, the smaller of the two positive roots, A_u, corresponds to unstable limit cycle; the larger root, A_s, corresponds to a stable limit cycle.

By increasing U, it is possible to reduce the stable limit cycle amplitude A_s, but only so much. The smallest possible $A_s = 2\sqrt{3}/3 = A_* \approx 1.15$ is achieved for $U = U_{max}$, when $A_s = A_u = A_*$. This means the fixed amplitude control allows reducing the oscillation amplitude at most by 42% (from $A = 2$ to $A_* = 1.15$). More advanced feedback control is discussed in the next section of this paper.

Figure 2 and the analysis in this subsection are based on (8). Amplitude dynamics (8) is obtained from the Van der Pol model, which is a grossly simplified model of the combustion instability. Yet, the general appearance of the $\dot{A}(A)$ curve in Figure 2 and the analysis of this subsection would hold for more complex nonlinear models of the thermo-acoustic instability. The conclusions would hold as well, perhaps, with different values of the parameters and amplitudes.

D. Phase dynamics

Now consider the phase dynamics (7) assuming the base frequency excitation, $w = \Omega$. Assume that the excitation phase is fixed, $\psi = 0$. Then phase dynamics (7) becomes

$$\dot{\phi} = \frac{a}{Aw}\sin\phi.$$

The state space for this equation is illustrated in Figure 3. There are two equilibria corresponding to $\sin\phi = 0$, the first $\phi = 0$ and the second $\phi = \pi$. For $0 < \phi < \pi$, the derivative $\dot{\phi}$ is positive and ϕ increases. For $\pi < \phi < 2\pi$, the derivative $\dot{\phi}$ is negative and ϕ decreases.

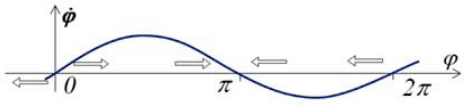

Fig. 3. Phase dynamics and its two equilibria

The first equilibrium $\phi = 0$ of the relative phase corresponds to maximum suppression of the instability and is, unfortunately, unstable. The second equilibrium $\phi = \pi$ corresponds to maximum enhancement of the instability by the forcing function (fuel modulation) and is stable. Thus, the phase control is a difficult problem of controlling an unstable system.

This is a fundamental property of the problem that can be seen from the most basic model of the externally excited oscillator. Yet, it appears that the unstable nature of the phase control problem was not recognized in the earlier literature.

III. Control Analysis

Phase shifting control requires knowledge of oscillation amplitude and phase. Section IV describes TED (Timing Error Detection) for the PLL (Phase Lock Loop) filter that provides an accurate estimate of oscillation amplitude and phase from noisy sensor data. The estimation introduces feedback delay. In addition to that, there are unavoidable transport delays for the fuel traveling from the modulation valve to the nozzle through the supply lines and from the nozzle to the combustion zone.

This section provides stability analysis of the phase shifting control taking the feedback delay into account. The averaged model (6), (7) is extended to include the delay.

A. Phase Control

The goal for controlling the phase of the fuel modulation is to maintain the phase that allows the best suppression of the combustion oscillations. Consider phase dynamics (7). The strategy is to keep the excitation frequency close to the oscillation frequency, $w \approx \Omega$. Assume that $w = \Omega$. Then $\phi = \psi$ is an equilibrium point for (7) and the strategy is to keep the phase ψ such that $\psi - \phi = 0$. This strategy obtains estimates of the frequency and phase from the TED-PLL estimator, see Section IV.

Control law: Let d be the control deadtime. At each time sample of the control, the control logic applies a fixed phase shift correction to the estimated combustion oscillation phase. The commanded excitation frequency $w_c(t)$ and the commanded excitation phase ψ_c are computed as

$$w_c(t) = \hat{w}(t) \quad (9)$$

$$\psi_c(t) = \hat{\phi}(t) + \delta \quad (10)$$

where $\hat{w}$ and $\hat{\phi}$ are the oscillation frequency and the phase estimates. The commanded excitation acts on the oscillations in the combustion process with delay d. Assuming that $\hat{w} = w = \text{const}$ and $\hat{\phi}(t) = \phi(t)$, the actual excitation phase is

$$\psi(t) = \psi_c(t-d) + wd = \phi(t-d) + \delta + wd, \quad (11)$$

If $\delta = -wd$, then we have $\psi(t) = \hat{\phi}(t-d) = \phi(t) = \text{const}$ and $\theta = \psi - \phi = 0$ as desired.

Closed loop dynamics: By substituting (11) and $\delta = -wd$ into (7) we get

$$\dot{\phi}(t) = \frac{\Omega^2 - w^2}{w} - \frac{a}{Aw}\sin(\phi(t-d) - \phi(t)) \quad (12)$$

To analyze the stability of this system, assume that the oscillation phase is $\phi(t) = qt + x(t)$, where q has the meaning of the shift in the oscillation frequency w that is caused by the phasing control. At the steady state we have $x(t) = 0$; hence, (7) yields

$$q = \frac{\Omega^2 - w^2}{w} + \frac{a}{Aw}\sin(qd)$$

Dynamics in variations for $x(t)$ in the vicinity of the steady regime $\phi(t) = qt$ is

$$\dot{x}(t) = -\frac{a}{Aw}\sin(x(t-d) - x(t))$$

The time scaling $\tau = t/d$ makes the deadtime d unity and yields a dynamical system $x' = -\gamma\sin(x(\tau-1) - x(\tau))$ that is characterized by a single nondimensional parameter $\gamma = ad/(Aw)$.

Stability analysis: Approximate analysis of the stability can be done by linearizing the system in the vicinity of the solution $x = \text{const}$ to get $x' = \gamma x(\tau) - \gamma x(\tau - 1)$. This delay system is of the form studied in [7]. Two conditions of its stability can be adopted from [7]. One stability condition is that $\gamma < 1$. Another asymptotic stability condition given in [7] is violated. Our system is on the stability boundary. Indeed, its characteristic equation $s = \gamma(1 - e^{-s})$ has a root $s = 0$. This root described the solution $x = \text{const}$ that is a neutral equilibrium and thus not asympotically stable. Any constant ϕ in (11), (12) can yield the desired phase shift $\theta = \psi - \phi = 0$. Thus, we get $\gamma < 1$ as the only condition of phase control stability that matters. In accordance with the definition of γ, this condition can be written as

$$ad < Aw \quad (13)$$

Stability condition (13) was derived for the linearized system. It tightly describes the stability boundary for the nonlinear system as well. Extensive nonlinear system simulations always give an apparently stable solution for $\gamma < 1$. Two out of the four parameters in (13) - frequency w, and control deadtime d - describe properties of the system. Parameters a and A are related to the control algorithm. One important conclusion that can be made from (13) is that the forcing (fuel modulation) intensity a must be small for small oscillation amplitude A to ensure the phase stability.

B. Amplitude control

Assume that the phase of the fuel flow modulation is locked to provide for the maximum suppression of the oscillations. Then, the amplitude dynamics (8) describe the rate of amplitude change depending on the control handle $U = 4a\cos\theta/(\mu\Omega)$, where a is the the fuel flow modulation

amplitude. Phase control maintains amplitude control efficiency by keeping θ close to zero. The phase estimation and control do not need to be especially precise for the amplitude control to work. Controlling the phase shift θ to be within ± 0.45 rad would keep $\cos\theta > 0.9$, which is sufficient.

Control law: The goal of amplitude control is to avoid eliminating oscillations altogether. Instead they have to be maintained at a small sustained level. One reason is that if the controlled oscillation amplitude becomes smaller than the noise, phase lock is lost and the forcing excites the oscillations instead of reducing them. Another reason is that phase control stability condition (13) is violated for small oscillation amplitude A.

The simplest control strategy is to maintain a fixed modulation amplitude, $U = \text{const}$. Subsection II-C explains that this strategy does not allow reducing oscillation amplitude below the theoretically smallest stable limit cycle of $A = 1.15$. Ideally, one would like to control the oscillations to a small level, e.g., 10% of the uncontrolled amplitude $A = 2$. In accordance with Subsection II-C, this is only possible by stabilizing the unstable equilibrium (unstable limit cycle) described in Subsection II-C.

Consider the problem of feedback stabilization of equilibrium A_u in (8). The linear feedback can be presented as

$$U_c(t) = U_u + F(\hat{A}(t) - A_u), \tag{14}$$

where F is the feedback gain and $\hat{A}(t)$ is the estimate of the oscillation amplitude obtained from the TED-PLL filter. The steady state control input is $U_u = 4A_u - A_u^3$. In practice, the exact value U_u corresponding to A_u can be provided by a slow integral term in a PI controller.

Closed loop dynamics: The commanded forcing acts on the oscillations in the combustion process with delay d. The actual forcing amplitude is then $U(t) = U_u + F(A(t - d) - A_u)$. By linearizing (8) around A_u and introducing the amplitude deviation $x(t) = A(t) - A_u$ we get the dynamics in variations

$$\dot{x}(t) = gx(t) - kx(t - d), \tag{15}$$

$$g = \frac{1}{4}\mu\Omega(4 - 3A_u^2), \quad k = \frac{1}{4}\mu\Omega F, \tag{16}$$

Stability analysis: The stability conditions for delay systems of the form (15) were studied earlier and are given by [7] as

$$dg < 1, \quad g < k < \sqrt{g^2 + \vartheta^2}, \tag{17}$$

where ϑ is a nonlinear function of the system parameters that is described in [7] and is unimportant for this analysis. The second condition in (17) can be satisfied by proper selection of the feedback gain F in (16). The condition $dg < 1$ deserves a more detailed analysis. Note that g in (16) depends on the target amplitude A_u. In case of $A_u \ll 1$, substituting g from (16) into (17) yields the condition $\mu < 1/(\Omega d)$. For example, if $\Omega = 2\pi \cdot 800$ Hz and $d = 0.011$ s, we get $\mu < 0.018$. This means the feedback control of very small oscillation amplitude is possible only if the instability growth rate is very weak.

IV. Estimation of Oscillation State

Implementation of the described control approaches requires estimates for the amplitude and phase of the combustion oscillations from the observed noisy sensor signal. TED (Timing Error Detection) form of the PLL (Phase Lock Loop) is used in advanced digital communication systems for similar purpose, e.g., see [16, Chapt. 6]. Use of a basic PLL in oscillation suppression control is discussed in [11]. We adopted TED-PLL to deal with the multirate data collection scheme in the experimental systems where a buffer containing 67 samples acquired at 0.06 ms interval is collected every 4ms.

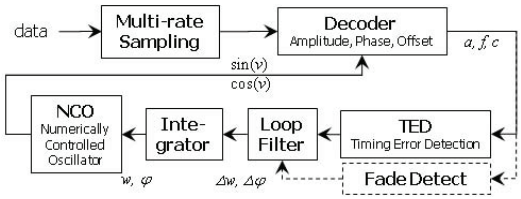

Fig. 4. Timing Error Detection (TED) phase tracking loop

A. TED-PLL

The standard design of the TED-PLL loop is illustrated in Figure 4. At sample k the inputs to the loop are: data time series Y (buffer content), past frequency estimate $w(k-1)$, and past phase estimate $f(k-1)$. The outputs are: updated frequency estimate $w(k)$, updated phase estimate $f(k)$, and amplitude estimate $a(k)$.

The Decoder works by solving a batch linear least squares model fit problem for data Y,

$$J = \min_{a,f,c} \sum_j [y(t_j) - a\sin(v_j + f) - c]^2, \tag{18}$$

where $y(t_j)$ are the sampled buffer data stored in Y and the phase sequence $v_j = w(k-1)t_j$ comes from the Numerically Controlled Oscillator (NCO).

The timing correction is done by Loop Filter and Integrator through update of $w(k)$ and $\phi(k)$. This update is the key part of the PLL. The state space formulation of this update is

$$w(k) = w(k-1) + (1-\alpha)T^{-1}f(k), \tag{19}$$

$$\phi(k) = w(k-1)T + \phi(k-1) + f(k), \tag{20}$$

where α is the filter tuning parameter and T is the filter update interval.

B. PLL Stability

To analyze TED-PLL tracking performance and the effects of loop feedback gain on the convergence assume that the buffer data Y covers exactly one sampling interval. Consider small deviations from the stationary point $w = w_*$, $\phi = 0$. Assuming ideal Decoder/TED, we get $f(k) = -\phi(k)$. The closed loop dynamics in variations then is

$$\begin{bmatrix} \tilde{w}(k) \\ \phi(k) \end{bmatrix} = \begin{bmatrix} 1 & -(1-\alpha)T^{-1} \\ 1 & 0 \end{bmatrix} \begin{bmatrix} \tilde{w}(k-1) \\ \phi(k-1) \end{bmatrix}, \tag{21}$$

where $\tilde{w}(k) = w(k) - w_*$. The characteristic values for (21) (the closed-loop poles) are $\lambda_{1,2} = 0.5 \pm \sqrt{-0.75 + \alpha}$. The fastest PLL convergence is achieved for the tuning parameter $\alpha = 0.75$; then, $\lambda_{1,2} = 0.5$. For heavy filtering and slow response, selecting α such that $0 < 1 - \alpha \ll 1$, yields $\lambda_1 \approx \alpha$ and $\lambda_2 \approx 1 - \alpha$. Our simulations and experiments used $\alpha = 0.75$.

C. Fade Detect

Fade Detect logic tests the Bayesian hypothesis that PLL lock is lost at this cycle: the signal has faded and no oscillations are detected. The fade (null) hypothesis H_0 assumes that the data just consists of noise. The lock hypothesis H_l assumes that the data contains oscillations and noise. Assuming the same additive white gaussian noise for both hypotheses yields the log-likelihood ratio

$$\begin{aligned} L &= \log \frac{P(H_l|Y)}{P(H_0|Y)} = \log \frac{P(Y|H_l)P(H_l)}{P(Y|H_0)P(H_0)} \\ &= \frac{\|Y\|^2 - J - 2\sigma^2\tau}{2\sigma^2}, \end{aligned}$$

where $\tau = \log[P(H_0)/P(H_l)]$ is the log-ratio of prior probabilities for the hypotheses, J is the optimal index in (18), and σ is the noise covariance. If $L > 0$ the signal is considered locked. If the signal has faded, $L \leq 0$; in that case TED-PLL propagates the old phase and frequency estimates to the next step without a correction. The Fade Detect logic has a single tuning parameter $r = 2\sigma^2\tau$.

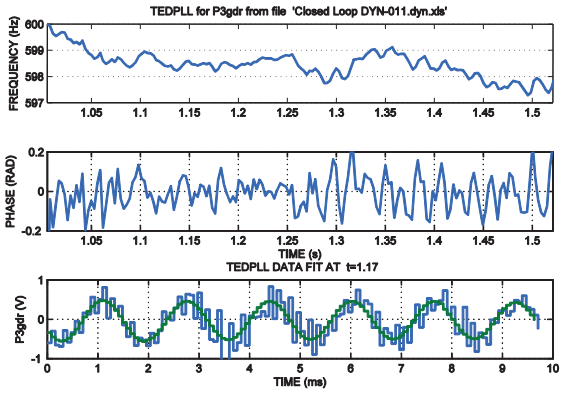

Fig. 5. TED PLL tracking of experimental data for acoustic sensor

D. Simulation

Further analysis and simulation demonstrate that the TED-PLL reliably converges for up to 30% error in the initial frequency and any initial phase error. It provides accurate frequency and phase estimates for signal amplitude 2-3 times smaller than the noise. For large noise, heavier filtering is required.

The TED-PLL algorithm was implemented and used in the experiments reported below. Figure 5 shows TED PLL tracking of experimental data from the acoustic sensor. The upper plot shows the frequency estimate through a 0.55 sec segment of the data; the middle plot shows the TED phase. The lower plot zooms in on 10 ms of the data around the middle of the segment and shows the estimate recovered by TED PLL along with the noisy raw signal from the sensor.

V. Simulation

A closed-loop simulation was developed in Simulink to verify the presented results of the control analysis. The experimental setup complete with the ACCS software logic was simulated. The simulation parameters were chosen to resemble the experimental system described further in Section VI. The simulation included the following main blocks.

Combustion Plant.: The simulation model describes the effects of thermo acoustic instability and fuel flow modulation using the model (1), (2), (3). The plant model includes the noise and delays in the acoustic and optical sensors. The model parameters varied for several rounds of experiments performed on different test rigs in this work. This study used the following representative set of simulation parameters: self-excitation intensity $\mu = 0.02$, frequency $\Omega/(2\pi) = 800$Hz, external forcing $a = gA_n$, where $g = 15,000$ and $A_n \leq 50$ psi is the amplitude of the nozzle pressure modulation. The control deadtime was $d = 11$ms. The acoustic pressure sensor gain is 3 when measuring the oscillation pressure $p(t)$. The simulation included state and measurements noise.

Actuator System.: Goodrich fuel flow valve described in [14] and its low level controls were simulated. The valve model includes the phased pulse-width modulation of the flow, deadtime, and filtering of the rectangular modulation pulses in the valve.

Control System.: The control system simulation includes the model of data acquisition. With its multirate sampling (oversampling). The sensor data is sampled at 16.6667 KHz rate (0.06 ms interval). Every 4ms, the buffer of the last 67 samples is processed to determine the amplitude, frequency, and phase of the oscillations. These are further used to compute the commanded amplitude, frequency, and phase of the modulation commanded to the actuators. The detail are described below.

Estimation Logic.: The TED-PLL loop was implemented for estimation of the oscillation state (phase and amplitude) as described in Section IV.

Feedback Control Logic.: An issue with the phase shifting strategy, which is not discussed in the literature on the subject, is that the fixed phase shift might not work if the process deadtime d (between the fuel flow modulation and its combustion impacts) is sufficiently large. This is because the active control causes a change Δw in oscillation frequency that leads to the phase change $\Delta f = \Delta w d$. For example, take deadtime $d = 10$ ms; then, the frequency change from 500Hz to 550Hz, $\Delta w = 50$Hz, yields phase change of π, which would render control unstable.

The strategy that we use to compensate for the frequency change is to select δ in (10) as $\delta = -\hat{w}\hat{d} + \tilde{\delta}$. Here $\hat{w}$ and $\hat{d}$ are the estimates of the frequency and the deadtime and $\tilde{\delta}$ is an empirical phase change compensating for the errors in determining w and d. Achieving $\delta = -wd$ requires that

$\tilde{\delta} = (\hat{w}-w)d+\bar{w}(\hat{d}-d)+(\hat{w}-\bar{w})(\hat{d}-d)$, where $\bar{w}$ is average value of the frequency in the experiment. The first term is small if the frequency estimate is accurate, the second term is fixed phase error that does not change with time, and the third term is much smaller than Δwd provided that $\hat{d}-d$ is much smaller than d. The described strategy was used in the simulation and in the experiments.

Simulation Results: Figure 6 shows the simulation results. The nondimensional oscillation amplitude A can be evaluated from the bottom plot for acoustic pressure amplitude. The amplitude is $A = 2P/P_0$, where P is the observed pressure amplitude and P_0 is the steady state pressure amplitude in the absence of control forcing. In the bottom plot of Figure 6, P_0 is the average value for the first second of the simulation.

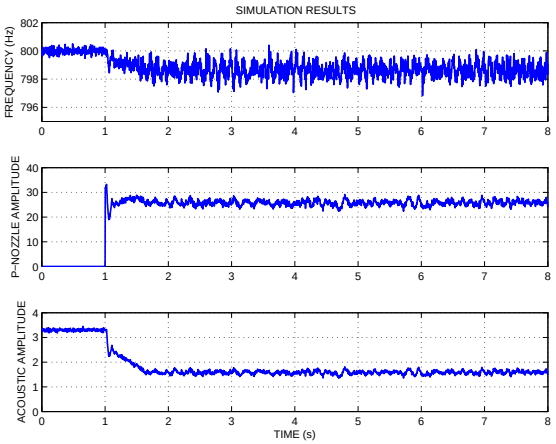

Fig. 6. Closed loop simulation with PI phase shifting controller

The simulation used realistic levels of observation and process noise that match the experimental data. In addition, the effective feedback delay is larger than the deadtime d by the TED-PLL estimator delay (another 6-9 ms added to $d = 11$ ms). With the noise, the transients, and the delays present in the simulation we were able to stabilize the oscillation amplitude $A_u = 0.97$. This is an unstable limit cycle (we have $A_u < A_*$), but the amplitude is not much smaller than $A_* = 1.15$.

The simulation had implemented a PI amplitude controller. The P controller given by (14) was completed by a small I term. Effectively the integrator accumulates the steady state offset U_u in (14) that is required to achieve the target amplitude. Phase control implemented in simulation followed (9), (10).

The upper plot in Figure 6 shows the time trace of the oscillation frequency in the simulation estimated using the TED-PLL filter described in Section IV. The middle plot displays the forcing control (the commanded nozzle pressure amplitude).

Though accurate identification of μ from the experimental data was not possible, there are indications that in experiments μ might be much larger than 0.02. This means a A_* cannot be practically stabilized in the experiments.

Discussion of simulation results.: The analysis of Section III provides a possible explanation why most of the published results of active combustion control experiments show about 50% reduction in the amplitude, very rarely more. The answer is that the combination of the control deadtime and instability growth rate does not permit stable control of the oscillations to smaller amplitudes.

For the system parameters $\Omega = 2\pi \cdot 800$ Hz, $d = 0.011$ s, and $\mu = 0.02$) the condition $dg < 1$ yields $1 - 0.75A_u^2 < 1/(\mu\Omega d) \approx 0.9$. This holds for $A_u > 0.36$. The minimal theoretically achievable limit cycle amplitude cannot be attained in practice. The transients and the noise present in the system require that the steady amplitude has a large domain of attraction. The theoretical limit can only be approached with a substantial margin.

VI. Experiments

A series of experiments were conducted with the described phase-shifting ACCS control logic.

A. Experimental setup

Several experimental setups and test rigs were used in this study. The experimental results described below were obtained in March 2010 tests on a combustor rig.

Combustor test rig: The combustor rig includes a pressurized flame tube providing realistic combustion conditions. It is outfitted with a single fuel injector produced for jet engines complete with Goodrich fuel modulation actuator described in [14]. In the experiments, the airflow was around 1800 lbm/hr, the rig pressure 180 psia, the temperature upstream of injector/combustor 575° F, and the fuel flow through the valve 180 lbm/hr. In the experiments with this setup, a thermo-acoustic instability was created at the frequency around 800 Hz. Unlike most of prior active combustion control work, our experiments were done under conditions that realistically emulated a jet engine combustor. This makes the control more challenging.

Actuator design and valve modulation: The Goodrich valve used for fuel modulation is described in [14]. The valve allows deep modulation (up to 30 %) of the fuel flow at the frequency of up to 1000 Hz. The pulse-width modulation applied to flow is smoothed by the fluid dynamics in the valve. The valve actuator design, calibration, and control present a separate set of engineering challenges that are outside the scope of this paper. The designed actuator control hardware and control logic were demonstrated to provide the desirable modulation of the fuel flow.

Sensor design: As described in [14], along with the Goodrich valve, there are several sensors integrated into the fuel injector. The sensors are designed for the jet engine combustor environment. The two optical combustion sensors (CH and OH) are looking downstream into the combustion zone. The two acoustic microphone sensors for measuring combustion pressure oscillations are situated upstream of air swirlers. The experiments described below, used an additional pressure sensor at the exit of the flame tube, This sensor corresponds to P4′ sensor in a jet engine. (P4 is the pressure at the high pressure turbine inlet).

Control logic: The control system implemented in the experiments includes the estimation logic and feedback control logic. It corresponds to the control system implemented in simulation and described in Section V.

B. Experimental results

A sample of the experimental results for phase and amplitude control is shown in Figure 7. The experiments used phase controller (9), (10) and the amplitude controller (14).

The bottom plot in Figure 7 shows the amplitude of the pressure oscillations estimated from acoustic sensor signal by TED-PLL. The upper plot shows the oscillation frequency obtained for the same pressure signal by TED-PLL. The middle plot shows the fuel pressure amplitude that describes the amplitude control. The light colored dots in Figure 7 show the actual PLL data and the solid line shows the smoothed data. We used a zero phase noncausal low-pass filter with 31 taps for plot smoothing.

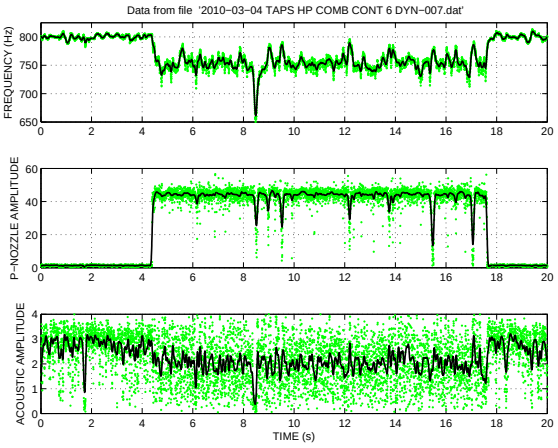

Fig. 7. Experimental results for phase and amplitude control

The upper plot in Figure 7 shows a strong change in the oscillation frequency with the forcing (almost 50 Hz). The frequency change is caused by nonlinear effects that are not captured in the simulation model; the frequency change in upper plot in Figure 6 is much smaller. This frequency change makes phase shifting control more challenging.

The observed thermo-acoustic oscillations were somewhat unstable because of the turbulent flow effects that provide a string colored noise excitation. This deviates from the simulation model that assumes a stable limit cycle and small white noise. This also causes periodic loss of PLL lock as the oscillation signal fades out and in. The unstable nature of the oscillations can be seen from the first 5 sec of the data in the plots before the fuel flow modulation starts.

Despite all the above issues, a consistent reduction of the oscillation amplitude was achieved with the phase shifting control. The amplitude reduction of about 31% is visible at the bottom plot in Figure 7. This reduction corresponds to the nondimensional amplitude $A = 1.38$. (For the sustained uncontrolled oscillations, $A = 2$). This is consistent with the analysis of Section III. The conclusion is that it is fundamentally difficult to achieve further reduction for a liquid fuel combustor system with these parameters

REFERENCES

[1] Annaswamy, A.M. and Ghoniem, A.F., "Active Control of Combustion Instability: Theory and Practice," *IEEE Control Systems Magazine*, Vol. 22, No. 6, 2002, pp. 37–54.

[2] Banaszuk, A., Ariyur, K.B., Krstic, M., and Jacobson, C.A., "An adaptive algorithm for control of combustion instability," *Automatica*, Vol. 40, 2004, pp. 1965–1972.

[3] Banaszuk, A., Mehta, P.G., Jacobson, C.A., and Khibnik, A.I. "Limits of achievable performance of controlled combustion processes," *IEEE Transactions on Control Systems Technology*, Vol. 14, No. 5, 2006, pp. 881–895.

[4] Bouziani, F., Landau, I.D., Bitmead, R.R., and Voda-Besancon, A. , "Analysis of a tractable model for combustion instability: the effect of delay and low pass filtering," *IEEE Conf. on Decision and Control*, Dec. 2006, San Diego, CA

[5] Bogolyubov, N.N. and Mitropol'skii, Yu.A., *Asymptotic methods in the theory of nonlinear oscillations*, Nauka, Moscow, 1974 (in Russian), Gordon and Breach, New York, 1964.

[6] Culley, D., Garg, S., Hiller, S.J., Horn, W., Kumar, A., Mathews, H.K., Moustapha, H., Pfoertner, H., Rosenfeld, T., Rybarik, P., Schadow, K., Stiharu, I., Viassolo, D.E., and Webster, J., *More Intelligent Gas Turbine Engines*, NATO RTO Report TR-AVT-128, 2009, Neuilly-Sur-Seine, France. Available: `http://handle.dtic.mil/100.2/ADA515458`

[7] Cooke, K.L. and Grossman, Z., "Discrete delay, distributed delay and stability switches," *Journ. of Mathemathical Analysis and Applications*, Vol. 86, 1982, pp. 592–627.

[8] F.E.C. Culick, "Combustion instabilities in liquid-fuelled propulsion systems: an overview", *AGARD-CP-450*, 1988. Available: `http://authors.library.caltech.edu/22028/1/307_Culick_FEC_1988.pdf`

[9] Dowling, A.P. and Morgans, A.S., "Feedback control of combustion oscillations," *Annual Review of Fluid Mechanics*, Vol. 37, 2005, pp. 151–182.

[10] Hermann, J., Orthmann, A., Hoffmann, S., and Berenbrink, P. "Combination of active instability control and passive measures to prevent combustion instabilities in a 260 mw heavy duty gas turbine," *NATO RTO/AVT Symposium on Active Control Technology for Enhanced Performance in Land, Air, and Sea Vehicles*, Braunschweig, Germany, May 2000.

[11] Guo X. and Bodson, M., "Analysis and implementation of an adaptive algorithm for the rejection of multiple sinusoidal disturbances," *IEEE Transactions on Control Systems Technology*, Vol.17, No. 1, 2009, pp. 40–50.

[12] Lovett, J.A., Teerlinck, K.A., and Cohen, J.M., *Demonstration of active combustion control*, NASA Report CR-2008-215491, December 2008

[13] Moran, A.J., Steele, D., Dowling, A.P., "Active control of combustion and its application, *NATO/RTO Spring 2000 Symposium on Active Control Technology for Enhanced Performance Operation Capabilities of Military Aircraft, Land Vehicles and Sea Vehicles*, Braunschweig, Germany, 2000.

[14] Myhre, D., Aadland, T. , Goeke, J., and Cornwell, M., "Integrating optical sensors in fuel injectors for combustion control," *ASME Turbo Expo*, June 9-13, 2008, Berlin, Germany, GT2008-51418.

[15] Neumeier, Y. and Zinn, B.T., "Experimental demonstration of active control of combustion instabilities using real-time modes observation and secondary fuel injection," *26th Int. Symp. on Combustion/The Combustion Institute Proc.*, Vol. 26, pp.2811–2818, 1996.

[16] Proakis, J.G., *Digital Communications*, 4th Ed., McGraw-Hill, New York, 2001.

[17] Sattinger, S.S., Neumeier, Y., Nabi, A., Zinn, B.T., Amos, D.J., and Darling, D.D., "Sub-scale demonstration of the active feedback control of gas-turbine combustion instabilities," *ASME Journal of Engineering for Gas Turbines and Power*, Vol. 122, pp. 262–268, 2000.

[18] Seume, J.R., Vortmeyer, N., Krause W., Hermann, J., et al "Application of active combustion instability control to a heavy duty gas turbine," *ASME Journal of Engineering for Gas Turbines and Power*, Vol. 120, pp. 721–726, 1998.